Flazin improves mitochondrial dynamics in renal tubular epithelial cells under oxidative stress

Xun-Zhi Wu[a,1], Hsin-Jung Ho[a,1], Miki Eguchi[a], Zhen Chen[a], Hitoshi Chiba[a,b], Shu-Ping Hui[a,*]

[a] Faculty of Health Sciences, Hokkaido University, Kita-12, Nishi-5, Kita-ku, Sapporo 060-0812, Japan

[b] Department of Nutrition, Sapporo University of Health Sciences, Nakanuma Nishi-4-2-1-15, Sapporo 007-0894, Japan

* Corresponding author, E-mail: keino@hs.hokudai.ac.jp, Tel.: +81-11-706-3693.

[1] These authors contributed equally to this work.

Abstract

Oxidative stress-induced mitochondrial disturbance plays a critical role in the progression of acute kidney injury and its transition to chronic kidney disease. Food-derived bioactive components have received long-lasting attention in nutraceutical therapy for various kidney diseases. Flazin is a food-derived β-carboline alkaloid widely discovered in fermented foods and fruit juice. In the present study, flazin was studied for its mitochondrial-improving effects on renal tubular epithelial HK-2 cells under oxidative stress. Flazin protected HK-2 cells from oxidative stress-induced cell death by reducing reactive oxygen species levels, decreasing mitochondrial-dependent apoptotic genes expression, and increasing antioxidative genes expression. Moreover, flazin improved mitochondrial dynamics by restoring mitochondrial branched structure and increasing length as well as network size through regulating fission/fusion-related genes expression. Flazin also improved the profile of mitochondria-specific phospholipid, cardiolipin, including increasing its content, improving its species, and reducing its hydroperoxides ratio through regulating cardiolipin biogenesis and remodeling genes expression. These resulted in increased ATP production and enhanced mitochondrial function. This study highlights the health-beneficial effect of flazin on cellular redox homeostasis and mitochondrial dynamics, suggesting it may serve as a daily nutraceutical to contribute to the prevention and treatment of kidney disease related to oxidative stress and mitochondrial disturbance.

Keywords

Flazin; Bioactive components; Oxidative stress; Mitochondrial disturbance; Kidney disease.

1. Introduction

Mitochondria are the energy source of cells, producing adenosine triphosphate (ATP) as the cellular energy currency to maintain metabolic homeostasis (Green & Reed, 1998). Along with ATP production, reactive oxygen species (ROS) are constantly generated as by-products, which are linked to mitochondrial function (Small et al., 2012). Oxidative stress occurs while ROS production extrapolates the cellular antioxidant system neutralizing capacity. It has been reported that persistently elevated ROS levels lead to mitochondrial disturbance, including damaged mitochondrial DNA and membrane permeability, decreased ATP production, increased cytochrome c release, and eventual apoptotic cell death (Chrysostomou et al., 2013; Guo et al., 2013). Recent studies have revealed that ROS-induced mitochondrial disturbance is associated with various diseases, including heart diseases (Federico et al., 2021), neurodegenerative diseases (Cherubini et al., 2020), and kidney diseases (Ho & Shirakawa, 2022).

The kidney is one of the highest energy-consuming organs and requires the second-highest mitochondrial density and oxygen consumption (Bhargava & Schnellmann, 2017; Ho & Shirakawa, 2022). Studies have indicated that mitochondrial ROS-induced oxidative stress plays a crucial role in the pathogenesis of acute kidney injury (AKI) and contribute to the transition of AKI to chronic kidney disease (CKD) (Basile et al., 2016; Gamboa et al., 2016). Oxidative stress causes renal cell loss and decreases the proliferative activity of renal cells, both involving mitochondrial disturbance (Small et al., 2012; Wang et al., 2022) Given the

54 critical role of mitochondrial oxidative stress in the onset and progression of AKI and CKD,
55 amelioration of oxidative stress and regain of mitochondrial homeostasis are considered
56 important therapeutic targets for the prevention and treatment of oxidative stress-related kidney
57 diseases (Bhatti et al., 2017; Song et al., 2022).

58 Food-derived bioactive components have long been used as a complementary therapy to
59 promote healthcare and treat kidney diseases due to their low treatment costs and minimal side
60 effects, such as resveratrol (Saldanha et al., 2016), quercetin (Hickson et al., 2019), and
61 curcumin (Emami et al., 2022). Flazin is a food-derived β-carboline alkaloid widely found in
62 fermented foods, such as sake, rice vinegar, and soy sauce (Nakatsuka et al., 1986), and fruit
63 juices, such as cherry tomato (Seong et al., 2021) and black currant (Makila et al., 2016). Recent
64 studies have claimed its protein glycation inhibiting (Seong et al., 2021), immunomodulatory
65 (Ying et al., 2021), and lipid metabolism-improving activities (Wu et al., 2022). Fuda *et al*. also
66 discovered the antioxidant effect of flazin in human hepatocytes (Fuda et al., 2019). However,
67 to the best of our knowledge, no study has investigated the effect of flazin on mitochondria in
68 kidney cells under oxidative stress.

69 To investigate if flazin has any effect on mitochondria in kidney cells under oxidative stress,
70 studies were designed and carried out. *In vitro* models of proximal tubular epithelial cell are
71 considered valuable alternatives to animal studies in renal disease research (Slyne et al., 2015).
72 L-buthionine-(S,R)-sulfoximine (BSO) is an inhibitor of γ-glutamylcysteine synthetase. It can
73 cause cellular glutathione depletion and induce oxidative stress (Cobbett et al., 1998). Thus,

74 BSO was added to human kidney proximal tubular epithelial HK-2 cells, and flazin was co-
75 incubated. This study aimed at investigating the effect of flazin on mitochondria dynamics in
76 HK-2 cells under oxidative stress.
77
78 **2. Materials and Methods**
79 **2.1. Chemicals and reagents**
80 Flazin was prepared and validated as described in our previous work (Fuda et al., 2019). Briefly,
81 2.18 mL $SOCl_2$ was added to 50 mL methanol (MeOH) dissolved with 10 mmol L-tryptophan.
82 After stirring overnight, NaOH aqueous solution was added to adjust the pH to 9-10 and the
83 solution was extracted by ethyl acetate. The extract was added to 10 mL CH_2Cl_2 containing 1
84 mmol 5-(hydroxymethyl)furfural, 80 μL trifluoroacetate, and 1 mmol of trichloroisocyanuric.
85 After 5-h reaction, the solution was extracted by ethyl acetate and the extract was dissolved in
86 5 mL MeOH containing 1mL NaOH aqueous solution (3 mol/L). The solution was heated to
87 65 °C for 5 h. Then, citric acid was added to adjust the pH to 4−5. Finally, the product was
88 extracted by ethyl acetate and purified with flash chromatography to give flazin. BSO and 2′,
89 7′- dichlorofluorescin diacetate (DCFH-DA) were purchased from Sigma-Aldrich (St. Louis,
90 MO, USA). For lipid extraction and analysis, LC-MS grade methyl tert-butyl ether (MTBE),
91 H_2O, MeOH, and isopropanol were purchased from Kanto Chemical Industry (Tokyo, Japan).
92 Cardiolipin (CL) 15:0/15:0/15:0/15:0 was synthesized in our previous study (Chen et al., 2020).
93 **2.2. Cell line and culture conditions**

HK-2 cells were obtained from American Type Culture Collection (Manassas, VA, USA) and cultured in Dulbecco's Modified Eagle's Medium (DMEM, Nacalai Tesque Kyoto, Japan) supplemented with 10% fetal bovine serum (FBS, Gibco, Grand Island, NY, USA), 1 U/mL penicillin-streptomycin solution (P/S, Fujifilm Wako, Osaka, Japan) in a 5% CO_2 humidified incubator at 37°C.

2.3. Cell viability assay

For investigating the effect of flazin against BSO treatment, cells were seeded into 96-well plates at a density of 3×10^3 cells/well. After overnight culture, the medium was replaced with DMEM (1% FBS and 1% P/S). BSO (100 μM) and flazin (7.8, 15.6, 31.3, and 62.5 μM) were introduced and incubated for 48h. Afterward, cell viability was tested with a cell counting kit-8 (CCK-8, Dojindo, Kumamoto, Japan) using a Wallac 1420 ARVO Mx plate reader (PerkinElmer, Tokyo, Japan). To further investigate the effect of flazin, concentrations of 31.3 and 62.5 μM were chosen for the following experiments.

2.4. Quantitative polymerase chain reaction (qPCR)

Cells were seeded into 6-well plates at a density of 5×10^4 cells/well. After overnight culture, media were replaced by DMEM (1% FBS and 1% P/S). BSO (100 μM) and flazin (31.3 and 62.5 μM) were added and incubated for 24 h. Afterward, cells were collected, and total RNA was isolated and purified by the TRIzol method (Invitrogen, Waltham, MA, USA). The concentrations and purities of RNA were determined using NanoDrop Microvolume Spectrophotometers (Thermo Fisher Scientific, Wilmington, DE, USA). RT-PCR was

performed using ReverTra Ace qPCR RT Master Mix (Toyobo Co., Ltd., Osaka, Japan). The gene expression level was determined by qPCR using a Step One Plus Real-Time PCR system (Applied Biosystems, Waltham, MA, USA) and Fast SYBR Green Master Mix (Applied Biosystems). The amplification conditions were as follows: 95°C for 3 min followed by 40 cycles of 95°C for 10 s and 60°C for 30 s. The relative expression levels of all genes were normalized to GAPDH and determined using the $2^{-\Delta\Delta CT}$ method. The primers used in the experiment, listed in Table S1, were synthesized by FASMAC (Kanagawa, Japan).

2.5. Intracellular ROS level measurement

Cells were seeded into black 96-well plates at a density of 3×10^3 cells/well. After overnight culture, the medium was replaced with DMEM (1% FBS and 1% P/S). BSO (100 μM) and flazin (31.3 and 62.5 μM) were added and incubated for 24 h. The intracellular ROS levels in HK-2 cells were determined by the oxidant-sensing fluorescent probe DCFH-DA. In brief, the cells were added with 25 μM DCFH-DA in 0% FBS DMEM at 37°C for 20 min and then washed twice with phosphate-buffered saline (PBS, Fujifilm Wako). The fluorescence was measured at Ex/Em: 485/535 nm using a Wallac 1420 ARVO Mx plate reader (PerkinElmer).

2.6. Fluorescence imaging

For morphological inspection, MitoTracker Green (Invitrogen) and Hoechst 33342 (Dojindo) were used to stain mitochondria and nuclei, respectively. Specifically, 1×10^5 cells/dish were seeded into the 35-mm dish (Iwaki, Tokyo, Japan) with DMEM (10% FBS and 1% P/S) and cultured overnight. The medium was removed and replaced by DMEM (1% FBS and 1% P/S).

BSO and flazin were added, and cells were treated for another 24 h. Before staining, the medium was replaced by DMEM (0% FBS, 1% P/S). Then, MitoTracker Green and Hoechst 33342 were introduced and incubated for 20 min. Afterward, the medium was removed and replaced by DMEM (1% FBS and 1% P/S). The stained cells were observed by a BZ-9000 All-in-one Fluorescence Microscope (KEYENCE, Osaka, Japan) with the excitation of 490 nm laser for MitoTracker Green and 350 nm laser for Hoechst 33342.

2.7. Lipid extraction

Cells were seeded into 6-well plates with 1.0×10^5 cells/ well. After overnight culture, the medium was replaced with DMEM (1% FBS and 1% P/S). BSO (100 μM) and flazin (31.3 and 62.5 μM) were added. Cells were treated for 24 h. After incubation, the medium was removed, and cells were rinsed with PBS. Then, cells were collected by a scraper and dissolved in 1 mL of PBS (0.1 mL for BCA assay and the rest for lipid extraction). BCA assay was conducted using the Pierce BCA Protein Assay Kit (Thermo Fisher Scientific) according to the manufacturer's instructions. For lipid extraction, total lipid was extracted according to the previously reported method (Matyash et al., 2008) with some modification. Briefly, cells in each tube were extracted twice with 900 μL of MTBE/MeOH/H_2O (6:2:1, v/v/v) and 128 pmol of CL 15:0/15:0/15:0/15:0 as internal standard. Afterward, the solvent system was centrifuged. The upper layer was collected, dried, and dissolved in MeOH. The obtained total lipid was stored in -80°C until analysis.

2.8. CL profiling

CL was profiled using a Prominence HPLC system (Shimadzu Corp., Kyoto, Japan) coupled to an LTQ Orbitrap mass spectrometer. The condition was according to our previous work (Chen et al., 2020). An Atlantis T3 C18 column (Waters, Milford, MA, USA) was used for lipids separation, and an electrospray ionization (ESI) source in negative mode was equipped for detection. The raw data were processed by Xcalibur 2.3 (Thermo Fisher Scientific), referring to the LIPIDMAPS database (www.lipidmaps.org, accessed on 11 November 2022) and our in-house library (Chen et al., 2020). The final result was normalized by total protein level. The amount of each CL species was calculated with the equation: $\text{Amount}_{\text{analyte}} = \text{Amount}_{\text{IS}} \times \text{Peak area}_{\text{analyte}}/\text{Peak area}_{\text{IS}}$. The total CL was calculated as the sum of all the CL species.

2.9. Intracellular ATP production test

HK-2 cells (3.0×10^3 cells/well) were seeded into a white 96-well plate in DMEM with 10% FBS and cultured overnight, followed by culturing with BSO and flazin in DMEM with 1% FBS for 24 h. Intracellular ATP level was tested using Cell ATP Assay Reagent (Toyo B-Net, Tokyo, Japan) following the manufacturer's protocol and was measured with a Wallac 1420 ARVO Mx plate reader (PerkinElmer).

2.10. Mitochondrial DNA copy number test

Cells were seeded into 6-well plates at a density of 5×10^4 cells/well. After overnight culture, media were replaced with DMEM (1% FBS and 1% P/S). BSO (100 μM) and flazin (31.3 and 62.5 μM) were introduced and incubated for 24 h. Afterward, total DNA was extracted and

purified using the NucleoSpin Tissue kit (Takara Bio., Shiga, Japan). Mitochondrial DNA copy number was relatively measured based on nuclear DNA using qPCR. Two primer pairs for detecting mitochondrial DNA and nuclear DNA were measured by Human Mitochondrial DNA Monitoring Primer Set (Takara Bio). The mitochondrial DNA copy number was calculated according to the manufactural instruction.

2.11. Statistical Analysis

All data are expressed as the mean ± standard deviation (S.D.) using GraphPad Prism 8 (GraphPad Software, Inc., La Jolla, CA, USA). Values were calculated using one-way analysis of variance (ANOVA) with the Tukey post hoc test. Different letters indicate significant difference and statistical significance was defined as $p < 0.05$.

3. Results and discussion

3.1. Flazin protected cells from oxidative stress-induced damage

Firstly, cytotoxicity of flazin was tested to determine the concentration used in the study. Flazin exhibited negligible cytotoxicity at concentrations below 62.5 μM (Fig. S1). Additionally, 31.3 and 62.5 μM flazin was found to improve ATP production of cells (Fig. S2). Given the strong correlation between ATP production and ROS level within cells, our interest was piqued regarding whether flazin has any effect on oxidative stress. To investigate whether flazin can protect cells against oxidative stress, cells were incubated with BSO and different doses of flazin. As shown in Fig. 1a, BSO treatment markedly decreased cell viability by 71.4% ± 13.5%.

194 The addition of flazin attenuated the decrease of cell viability in a dose-dependent manner.
195 Compared with the BSO group, flazin of 15.6 μM, 31.3 μM, and 62.5 μM increased cell
196 viability by 33.4% ± 12.1%, 43.0% ± 6.6%, and 56.2% ± 9.1%, respectively. No significant
197 difference was found between the control group and BSO + 62.5 μM flazin group, indicating
198 that 62.5 μM flazin can effectively protect cells from BSO-induced damage.

199 In addition to cell viability, the damage-related mRNA expressions were also tested to
200 determine the effect of flazin. BCL2-interacting killer (BIK) and Endonuclease-G (ENDOG)
201 play a role in mitochondrial-dependent apoptosis that can be considered markers of
202 mitochondrial damage (Mathai et al., 2005; Parrish et al., 2003). BIK is localized in the
203 endoplasmic reticulum and mediates apoptosis signaling to mitochondria (Hatzimichael et al.,
204 2012). ENDOG, a proapoptotic protein located in mitochondria, is released from mitochondria
205 and transported to the nucleus to induce cell death via DNA fragmentation during apoptosis (L.
206 Y. Li et al., 2001). The mRNA expressions of *BIK* and *ENDOG* were shown in Fig. 1b. BSO
207 treatment remarkably upregulated *BIK* and *ENDOG* expression levels (3.5-fold and 5.9-fold,
208 respectively). Comparatively, cells incubated with flazin showed decreased *BIK* and *ENDOG*
209 levels. These results indicated that flazin could effectively protect cells from BSO-induced cell
210 death.

211 **3.2. Flazin reduced intracellular ROS level**

212 Moderate ROS level is vital for cellular redox state and is essential in the physiological
213 regulation of intracellular signaling pathways (Finkel, 2011). However, the depletion of cellular

glutathione levels causes ROS accumulation and leads to oxidative stress in BSO-induced cells (Cobbett et al., 1998). Intracellular ROS level was tested by recruiting the cell-permeant reagent DCFH-DA as an indicator (Fig. 2a). Weak green fluorescence was observed in the control group, indicating a moderate level of ROS. BSO treated group exhibited strong green fluorescence, suggesting large amounts of ROS accumulated in cells. When flazin was added, fluorescence was evidently diminished with the increasing concentration of flazin. By calculating the fluorescence intensity, the quantitative result of the ROS level was shown in Fig. 2b. Compared with the control group, BSO treatment increased cellular ROS level by 26.4% ± 9.0%. When flazin was added, cellular ROS level decreased in a dose-dependent manner. Flazin of 31.3 and 62.5 μM decreased cellular ROS levels to normal levels as tested in the control group, indicating the ROS-lowering effect of flazin. To further investigate the antioxidant activity of flazin, antioxidant gene expressions were tested. Superoxide dismutase (SOD) is one of the key enzymes in the phase I antioxidant system, which converts superoxide to oxygen and hydrogen peroxide (Ighodaro & Akinloye, 2018). In human tissue, the *SOD1* gene encodes Cu/Zn-SOD localized in the cytosol, and the *SOD2* gene encodes MnSOD presented in mitochondria (Zelko et al., 2002). Catalase (CAT) is a common enzyme which catalyzes the transformation of hydrogen peroxide to water and oxygen (Ighodaro & Akinloye, 2018). The mRNA expression of *SOD1, SOD2*, and *CAT* was tested (Fig. 2c). BSO treatment cause negligible effect on *SOD1* and *SOD2* mRNA expression. In comparison, the addition of flazin significantly increased *SOD1, SOD2*, and *CAT* mRNA expression in a dose-dependent

manner. These results indicated that flazin could improve *SOD1, SOD2*, and *CAT* mRNA expression. Together, the mRNA expression of damage markers and antioxidant genes suggested that flazin can protect cells from BSO-induced oxidative stress by promoting antioxidant genes expression and inhibiting apoptotic genes expression.

3.3. Flazin preserved mitochondrial morphology

Mitochondria are the primary source of ROS and the immediate target of ROS damage (Bullon et al., 2014). Oxidative stress causes substantial changes to mitochondrial morphology, thereby interfering with its function (RJ & AM., 2014). Selective staining and microscopic inspection of mitochondria can provide important information about their morphological characteristics and overall state. In this study, MitoTracker Green was recruited to label mitochondria (Fig. 3a). In the control group, mitochondria exhibited reticulated networks with branched structures. In cells treated with BSO, fragmented and punctiform mitochondria were found. By contrast, when flazin was added, especially 62.5 μM flazin, mitochondria regained elongated and tubular shape. Besides, flazin treatment also rebuilt the mitochondrial network. Quantitative analysis of mitochondrial morphology was also conducted by calculating the mitochondrial length and network size (Fig. 3b and 3c). BSO markedly decreased the mean length and mean network size of mitochondria. Flazin treatment, especially 62.5 μM flazin, significantly increased the length and network size to the control level. It was reported that oxidative stress can result in the imbalance between fusion and fission, cause mitochondrial fragmentation, and induce apoptotic cell death (RJ & AM., 2014; Zheng et al., 2022). In cells

254 treated with flazin and BSO, mitochondria tended to fuse and regain elongation and network
255 structure, suggesting that flazin can inhibit mitochondrial fragmentation from BSO-induced
256 oxidative stress and contribute to mitochondrial fusion. Various beneficial effects of fused
257 mitochondrial states have been reported, such as increased ATP production, protection against
258 apoptosis, and extended cellular proliferation (Mitra, 2013; Zhao et al., 2017). Furthermore, as
259 in the stress state, improved quality control is significant to its physiological functions
260 (Hoitzing et al., 2015). These results indicated that flazin protected mitochondria dynamics
261 from BSO-induced oxidative stress and preserved mitochondrial morphology.

262 The coordination of fusion and fission plays a pivotal role in maintaining the mitochondrial
263 network (Song et al., 2022). Fission is mediated by dynamin-related protein 1(DRP1) and
264 mitochondrial fission 1 protein (FIS1), while fusion of mitochondrial inner membrane is
265 regulated by optic atrophy protein 1 (OPA1) (Lee et al., 2004). The mRNA expression levels
266 of these genes are shown in Fig. 3d. For the fission-related genes, both *DRP1* and *FIS1* were
267 upregulated by BSO treatment. When flazin was added, mRNA expression of *DRP1* and *FIS1*
268 were both downregulated in a dose-dependent manner. For the fusion-related gene, BSO
269 treatment did not affect mRNA expression of *OPA1*, whereas 62.5 μM flazin increased *OPA1*
270 expression significantly. The upregulation of *DRP1* and *FIS1* in BSO-treated cells indicated
271 the enhancement of mitochondrial fission, which is in line with the fragmentation of
272 mitochondria observed in mitochondrial staining (Fig. 3a). Cells treated with BSO and 62.5
273 μM flazin showed downregulated *DRP1* and *FIS1* mRNA expression with upregulated *OPA1*

mRNA expression, indicating the inhibition of fission and promotion of fusion. These results also followed the extensive interconnected membrane network seen in cells treated with BSO and 62.5 μM flazin, as shown in Fig. 3a. Collectively, these results indicated that flazin preserves mitochondrial morphology in cells under oxidative stress by regulating fission- and fusion-related genes expression.

3.4. Flazin improved CL profile

Cardiolipin (CL) is a mitochondria-specific phospholipid, which constitutes 15-20% of the inner mitochondrial membrane (Sifuentes & Lechleiter, 2018) and plays pleiotropic roles in mitochondria, including mitochondrial biogenesis, morphological maintenance, protein transport, and respiration process (Ho & Shirakawa, 2022; Ren et al., 2014). CL plays a central role in mitochondrial structure and function. However, oxidative stress enhances the formation of oxidized CL, contributing to mitochondrial injury (Yan et al., 2022). To evaluate the effect of flazin on CL in cells under oxidative stress, cellular lipids were extracted, and CL was analyzed. As shown in Fig. 4a, compared with the control group, BSO had less effect on total CL content, whereas 31.3 μM and 62.5 μM of flazin significantly increased total CL content by 22.3% ± 6.0% and 30.2% ± 16%, respectively. CL is an integral constituent of the mitochondrial inner membrane. A high CL content is essential for maintaining critical mitochondrial function, such as cristae formation and stabilization of respiratory complexes (Böttinger et al., 2012). Additionally, increasing CL content contributes to mitochondrial membrane fluidity, which is vital for mitochondrial architecture, respiration activity, and

protein transportation (Unsay et al., 2013).

CL is particularly vulnerable to oxidative stress due to its high content of easily oxidized unsaturated side chains and its location in the inner mitochondrial membrane near the ROS production site (Paradies et al., 2011). The main oxidized product of CL is CL hydroperoxides (CLOOH) (Pope et al., 2008). Total CLOOH content of cells with different treatments is shown in Fig. 4b. BSO treatment markedly increased CLOOH content compared with the control group. Compared with cells only treated with BSO, the addition of flazin exerted less influence on total CLOOH content. However, it significantly decreased CLOOH to CL ratio in a dose-dependent manner (Fig. 4c). These results indicated that flazin could significantly decrease the CLOOH ratio. Oxidation of CL disturbs its microdomain in the inner membrane, impairs its function of cristae maintenance and supercomplexes formation, and thus leads to mitochondrial dysfunction and cell death (Pope et al., 2008). Thus, redox homeostasis of CL is important for mitochondrial function maintenance and cell survival. Flazin effectively reduced the CLOOH ratio and restored redox homeostasis of CL, which is of great significance to the maintenance of mitochondrial structure and function.

In addition to total CL and CLOOH content, individual CL species also attracted our attention. As shown in Fig. 4d, BSO caused substantial changes to the CL profile. Generally, BSO treatment increased short-chain CL (such as CL 66:3, 66:4, 68:2, 68:3, 68:4, and 68:5) but decreased long-chain CL (such as CL 70:5, 70:6, 72:4, 72:5, 72:6, and 72:8). Comparatively, the addition of flazin reversed these changes induced by BSO. It decreased short-chain CL as

well as increased long-chain CL. The fatty acyl composition of CL was also elucidated according to the MS/MS fragmentation. As shown in Fig. 4e, compared with the control group, BSO treatment increased fatty acyl 16:0 and 16:1 but decreased fatty acyl 18:1 and 18:2. By contrast, the addition of flazin reversed these alterations. The alteration of the fatty acid chain of CL is intricately associated with CL oxidation (Ducasa et al., 2019). It is reported that linoleic acid (fatty acid 18:2) is preferentially incorporated into CL, resulting in increased CL 72:8, which is indicated to enhance mitochondrial function (Mulligan et al., 2012; Oemer et al., 2021). Mitochondria is the prominent source of ROS within the cell. The improved mitochondria function may contribute to the lowered ROS level (Indran et al., 2011). Collectively, flazin increased total CL content, decreased CLOOH ratio, reversed CL species disturbance, and improved CL fatty acyl chain composition, indicating that flazin can attenuate BSO-induced CL disturbance and improve CL profile, which can contribute to the improvement of mitochondrial morphology and function.

To investigate the mechanism of the improving effect of flazin on CL profile, expressions of enzymes involved in CL biogenesis and remodeling were tested. Cytidine diphosphate diacylglycerol synthase 1 and 2 (encoded by *CDS1* and *CDS2*), and phosphatidylglycerophosphate synthase 1 (*PGS1*), participate in CL biogenesis. The remodeling of CL depends on the activity of tafazzin (*TAZ*) (Schlame, 2013). The mRNA expression levels of the genes were shown in Fig. 4f. BSO treatment exerted less effect on CL biogenesis-related genes, while flazin upregulated the expression of these three genes. For CL

334 remodeling-related gene, 62.5 μM flazin significantly upregulated mRNA expression of *TAZ*.
335 These results indicated that flazin could improve CL profile by promoting CL biogenesis and
336 remodeling genes expression.

337 **3.5. Flazin increased ATP production**

338 An improved CL profile contributes to the formation of mitochondrial cristae, resulting in
339 more efficient ATP production (Mulligan et al., 2012). As flazin improved mitochondrial
340 dynamics, we are interested in whether the mitochondrial function was improved. Intracellular
341 ATP level was tested, and results were shown in Fig. 5a. BSO treatment markedly decreased
342 intracellular ATP level by 44.5 ± 4.0%. Comparatively, 31.3 μM and 62.5 μM flazin
343 significantly increased ATP levels by 49.5 ± 14.0% and 70.3 ± 15.4%, respectively. These
344 results indicated that flazin significantly improved ATP production in the cells. To further
345 investigate if the improving effect was induced by the improving mitochondrial dynamics, the
346 mitochondrial DNA copy number was then tested. As shown in Fig. 5b, both BSO and flazin
347 intervention cause less change to mitochondrial DNA copy number, indicating that BSO and
348 flazin exerted less effect on mitochondrial content. This result excluded the effect of
349 mitochondrial content on intracellular ATP levels in cells with different treatments. Collectively,
350 flazin can increase ATP production, which ascribes to improved mitochondrial dynamics.

351 As this study was carried out based on a cell model, further *in vivo* study is needed to clarify
352 its potential in treating oxidative stress-related kidney disease. Li et al. indicated that flazin is
353 orally bioavailable by ADME (absorption, distribution, metabolism, and excretion) simulation

in silico (H. Li et al., 2016). Considering these factors, the *in vivo* study is worth looking forward to.

4. Conclusions

This study is the first to discover the mitochondrial-improving effect of flazin in HK-2 cells under oxidative stress. Considering the health-beneficial effects of flazin in antioxidation and mitochondrial improvement, it may serve as a nutraceutical candidate to contribute to the treatment of oxidative stress-induced mitochondria disturbance in cells.

Authorship statement

Xun-Zhi Wu: Investigation, Data curation, Formal Analysis, Funding acquisition, Software, Validation, Writing – original draft. Hsin-Jung Ho: Conceptualization, Investigation, Data curation, Formal Analysis, Methodology, Software, Validation, Writing – original draft. Miki Eguchi: Investigation, Formal Analysis. Zhen Chen: Methodology, Writing – review & editing. Hitoshi Chiba: Conceptualization, Project administration, Writing – review & editing. Shu-Ping Hui: Conceptualization, Funding acquisition, Project administration, Writing – review & editing.

Declaration of competing interest

The authors declare no conflict of interests.

Acknowledgments

This work was supported by Japan Society for the Promotion of Science (JSPS) KAKENHI, Grant Number 19K07861, 23K06861, and JST SPRING, Grant Number JPMJSP2119.

Data availability

Data will be made available on request.

References

Basile, D. P., Bonventre, J. V, Mehta, R., Nangaku, M., Unwin, R., Rosner, M. H., Kellum, J. A., & Ronco, C. (2016). Progression after AKI: understanding maladaptive repair processes to predict and identify therapeutic treatments. *Journal of the American Society of Nephrology*, *27*(3), 687–697.

Bhargava, P., & Schnellmann, R. G. (2017). Mitochondrial energetics in the kidney. *Nature Reviews Nephrology*, *13*(10), 629–646.

Bhatti, J. S., Bhatti, G. K., & Reddy, P. H. (2017). Mitochondrial dysfunction and oxidative stress in metabolic disorders—A step towards mitochondria based therapeutic strategies. *Biochimica et Biophysica Acta (BBA)-Molecular Basis of Disease*, *1863*(5), 1066–1077.

Böttinger, L., Horvath, S. E., Kleinschroth, T., Hunte, C., Daum, G., Pfanner, N., & Becker, T. (2012). Phosphatidylethanolamine and cardiolipin differentially affect the stability of mitochondrial respiratory chain supercomplexes. In *Journal of Molecular Biology* (Vol.

423, Issue 5, pp. 677–686). https://doi.org/10.1016/j.jmb.2012.09.001

Bullon, P., Newman, H. N., & Battino, M. (2014). Obesity, diabetes mellitus, atherosclerosis and chronic periodontitis: a shared pathology via oxidative stress and mitochondrial dysfunction? *Periodontology 2000*, *64*(1), 139–153.

Chen, Z., Liang, Q., Wu, Y., Gao, Z., Kobayashi, S., Patel, J., Li, C., Cai, F., Zhang, Y., Liang, C., Chiba, H., & Hui, S. P. (2020). Comprehensive lipidomic profiling in serum and multiple tissues from a mouse model of diabetes. In *Metabolomics* (Vol. 16, Issue 11). https://doi.org/10.1007/s11306-020-01732-9

Cherubini, M., Lopez-Molina, L., & Gines, S. (2020). Mitochondrial fission in Huntington's disease mouse striatum disrupts ER-mitochondria contacts leading to disturbances in Ca2+ efflux and Reactive Oxygen Species (ROS) homeostasis. *Neurobiology of Disease*, *136*, 104741.

Chrysostomou, V., Rezania, F., Trounce, I. A., & Crowston, J. G. (2013). Oxidative stress and mitochondrial dysfunction in glaucoma. *Current Opinion in Pharmacology*, *13*(1), 12–15.

Cobbett, C. S., May, M. J., Howden, R., & Rolls, B. (1998). The glutathione-deficient, cadmium-sensitive mutant, cad2–1, of Arabidopsis thaliana is deficient in γ-glutamylcysteine synthetase. *The Plant Journal*, *16*(1), 73–78.

Ducasa, G. M., Mitrofanova, A., & Fornoni, A. (2019). Crosstalk Between Lipids and Mitochondria in Diabetic Kidney Disease. In *Current Diabetes Reports* (Vol. 19, Issue

12). https://doi.org/10.1007/s11892-019-1263-x

Emami, E., Heidari-Soureshjani, S., & Sherwin, C. M. T. (2022). Anti-inflammatory response to curcumin supplementation in chronic kidney disease and hemodialysis patients: A systematic review and meta-analysis. *Avicenna Journal of Phytomedicine*, *12*(6), 576.

Federico, M., De la Fuente, S., Palomeque, J., & Sheu, S. (2021). The role of mitochondria in metabolic disease: a special emphasis on heart dysfunction. *The Journal of Physiology*, *599*(14), 3477–3493.

Finkel, T. (2011). Signal transduction by reactive oxygen species. In *Journal of Cell Biology* (Vol. 194, Issue 1, pp. 7–15). https://doi.org/10.1083/jcb.201102095

Fuda, H., Miyanaga, S., Furukawa, T., Umetsu, S., Joko, S., Roan, Y., Suzuki, H., Hui, S.-P., Watanabe, M., & Chiba, H. (2019). Flazin as a promising Nrf2 pathway activator. *Journal of Agricultural and Food Chemistry*, *67*(46), 12844–12853.

Gamboa, J. L., Billings IV, F. T., Bojanowski, M. T., Gilliam, L. A., Yu, C., Roshanravan, B., Roberts, L. J., Himmelfarb, J., Ikizler, T. A., & Brown, N. J. (2016). Mitochondrial dysfunction and oxidative stress in patients with chronic kidney disease. *Physiological Reports*, *4*(9), e12780.

Green, D. R., & Reed, J. C. (1998). Mitochondria and apoptosis. *Science*, *281*(5381), 1309–1312.

Guo, C., Sun, L., Chen, X., & Zhang, D. (2013). Oxidative stress, mitochondrial damage and neurodegenerative diseases. *Neural Regeneration Research*, *8*(21), 2003.

Hatzimichael, E., Dasoula, A., Kounnis, V., Benetatos, L., Nigro, C. Lo, Lattanzio, L., Papoudou-Bai, A., Dranitsaris, G., Briasoulis, E., & Crook, T. (2012). Bcl2-interacting killer CpG methylation in multiple myeloma: A potential predictor of relapsed/refractory disease with therapeutic implications. In *Leukemia and Lymphoma* (Vol. 53, Issue 9, pp. 1709–1713). https://doi.org/10.3109/10428194.2012.661854

Hickson, L. J., Prata, L. G. P. L., Bobart, S. A., Evans, T. K., Giorgadze, N., Hashmi, S. K., Herrmann, S. M., Jensen, M. D., Jia, Q., & Jordan, K. L. (2019). Senolytics decrease senescent cells in humans: Preliminary report from a clinical trial of Dasatinib plus Quercetin in individuals with diabetic kidney disease. *EBioMedicine*, *47*, 446–456.

Ho, H.-J. J., & Shirakawa, H. (2022). Oxidative Stress and Mitochondrial Dysfunction in Chronic Kidney Disease. *Cells*, *12*(1), 88. https://doi.org/10.3390/cells12010088

Hoitzing, H., Johnston, I. G., & Jones, N. S. (2015). What is the function of mitochondrial networks? A theoretical assessment of hypotheses and proposal for future research. *Bioessays*, *37*(6), 687–700.

Ighodaro, O. M., & Akinloye, O. A. (2018). First line defence antioxidants-superoxide dismutase (SOD), catalase (CAT) and glutathione peroxidase (GPX): Their fundamental role in the entire antioxidant defence grid. *Alexandria Journal of Medicine*, *54*(4), 287–293.

Indran, I. R., Hande, M. P., & Pervaiz, S. (2011). hTERT Overexpression Alleviates Intracellular ROS Production, Improves Mitochondrial Function, and Inhibits ROS-

Mediated Apoptosis in Cancer CellshTERT, Mitochondria, and ROS. *Cancer Research*, *71*(1), 266–276.

Lee, Y., Jeong, S.-Y., Karbowski, M., Smith, C. L., & Youle, R. J. (2004). Roles of the mammalian mitochondrial fission and fusion mediators Fis1, Drp1, and Opa1 in apoptosis. *Molecular Biology of the Cell*, *15*(11), 5001–5011.

Li, H., Zhao, M., Su, G., Lin, L., & Wang, Y. (2016). Effect of soy sauce on serum uric acid levels in hyperuricemic rats and identification of flazin as a potent xanthine oxidase inhibitor. *Journal of Agricultural and Food Chemistry*, *64*(23), 4725–4734. https://doi.org/10.1021/acs.jafc.6b01094

Li, L. Y., Luo, X., & Wang, X. (2001). Endonuclease G is an apoptotic DNase when released from mitochondria. In *Nature* (Vol. 412, Issue 6842, pp. 95–99). https://doi.org/10.1038/35083620

Makila, L., Laaksonen, O., Alanne, A.-L., Kortesniemi, M., Kallio, H., & Yang, B. (2016). Stability of hydroxycinnamic acid derivatives, flavonol glycosides, and anthocyanins in black currant juice. *Journal of Agricultural and Food Chemistry*, *64*(22), 4584–4598.

Mathai, J. P., Germain, M., & Shore, G. C. (2005). BH3-only BIK regulates BAX,BAK-dependent release of Ca2+ from endoplasmic reticulum stores and mitochondrial apoptosis during stress-induced cell death. In *Journal of Biological Chemistry* (Vol. 280, Issue 25, pp. 23829–23836). https://doi.org/10.1074/jbc.M500800200

Matyash, V., Liebisch, G., Kurzchalia, T. V., Shevchenko, A., & Schwudke, D. (2008). Lipid

474 extraction by methyl-terf-butyl ether for high-throughput lipidomics. *Journal of Lipid*
475 *Research*, *49*(5), 1137–1146. https://doi.org/10.1194/jlr.D700041-JLR200
476 Mitra, K. (2013). Mitochondrial fission-fusion as an emerging key regulator of cell
477 proliferation and differentiation. *Bioessays*, *35*(11), 955–964.
478 Mulligan, C. M., Sparagna, G. C., Le, C. H., De Mooy, A. B., Routh, M. A., Holmes, M. G.,
479 Hickson-Bick, D. L., Zarini, S., Murphy, R. C., Xu, F. Y., Hatch, G. M., McCune, S. A.,
480 Moore, R. L., & Chicco, A. J. (2012). Dietary linoleate preserves cardiolipin and
481 attenuates mitochondrial dysfunction in the failing rat heart. In *Cardiovascular Research*
482 (Vol. 94, Issue 3, pp. 460–468). https://doi.org/10.1093/cvr/cvs118
483 Nakatsuka, S., Feng, B., Goto, T., & Kihara, K. (1986). Structures of flazin and YS, highly
484 fluorescent compounds isolated from japanese soy sauce. *Tetrahedron Letters*, *27*(29),
485 3399–3402. https://doi.org/https://doi.org/10.1016/S0040-4039(00)84806-6
486 Oemer, G., Edenhofer, M. L., Wohlfarter, Y., Lackner, K., Leman, G., Koch, J., Cardoso, L.
487 H. D., Lindner, H. H., Gnaiger, E., Dubrac, S., Zschocke, J., & Keller, M. A. (2021).
488 Fatty acyl availability modulates cardiolipin composition and alters mitochondrial
489 function in HeLa cells. In *Journal of Lipid Research* (Vol. 62).
490 https://doi.org/10.1016/J.JLR.2021.100111
491 Paradies, G., Petrosillo, G., Paradies, V., & Ruggiero, F. M. (2011). Mitochondrial
492 dysfunction in brain aging: role of oxidative stress and cardiolipin. *Neurochemistry*
493 *International*, *58*(4), 447–457.

494 Parrish, J. Z., Yang, C., Shen, B., & Xue, D. (2003). CRN-1, a Caenorhabditis elegans FEN-1
495 homologue, cooperates with CPS-6/EndoG to promote apoptotic DNA degradation. In
496 *EMBO Journal* (Vol. 22, Issue 13, pp. 3451–3460).
497 https://doi.org/10.1093/emboj/cdg320
498 Pope, S., Land, J. M., & Heales, S. J. R. (2008). Oxidative stress and mitochondrial
499 dysfunction in neurodegeneration; cardiolipin a critical target? In *Biochimica et*
500 *Biophysica Acta - Bioenergetics* (Vol. 1777, Issues 7–8, pp. 794–799).
501 https://doi.org/10.1016/j.bbabio.2008.03.011
502 Ren, M., Phoon, C. K. L., & Schlame, M. (2014). Metabolism and function of mitochondrial
503 cardiolipin. In *Progress in Lipid Research* (Vol. 55, Issue 1, pp. 1–16).
504 https://doi.org/10.1016/j.plipres.2014.04.001
505 RJ, Y., & AM., van der B. (2014). Mitochondrial fission, fusion, and stress. In *Science.*
506 *2012* (Vol. 337, Issue 6098, pp. 1062-5.).
507 Saldanha, J. F., Leal, V. O., Rizzetto, F., Grimmer, G. H., Ribeiro-Alves, M., Daleprane, J.
508 B., Carraro-Eduardo, J. C., & Mafra, D. (2016). Effects of resveratrol supplementation
509 in Nrf2 and NF-κB expressions in nondialyzed chronic kidney disease patients: a
510 randomized, double-blind, placebo-controlled, crossover clinical trial. *Journal of Renal*
511 *Nutrition*, *26*(6), 401–406.
512 Schlame, M. (2013). Cardiolipin remodeling and the function of tafazzin. In *Biochimica et*
513 *Biophysica Acta - Molecular and Cell Biology of Lipids* (Vol. 1831, Issue 3, pp. 582–

588). https://doi.org/10.1016/j.bbalip.2012.11.007

Seong, S. H., Jung, H. A., & Choi, J. S. (2021). Discovery of Flazin, an Alkaloid Isolated from Cherry Tomato Juice, As a Novel Non-Enzymatic Protein Glycation Inhibitor via in Vitro and in Silico Studies. *Journal of Agricultural and Food Chemistry*, *69*(12), 3647–3657. https://doi.org/10.1021/acs.jafc.0c07486

Sifuentes, M. M., & Lechleiter, J. D. (2018). Thyroid Hormone Stimulation of Adult Brain Fatty Acid Oxidation. In *Vitamins and Hormones* (Vol. 106, pp. 163–193). https://doi.org/10.1016/bs.vh.2017.05.006

Slyne, J., Slattery, C., McMorrow, T., & Ryan, M. P. (2015). New developments concerning the proximal tubule in diabetic nephropathy: in vitro models and mechanisms. *Nephrology Dialysis Transplantation*, *30*(suppl_4), iv60–iv67.

Small, D. M., Bennett, N. C., Roy, S., Gabrielli, B. G., Johnson, D. W., & Gobe, G. C. (2012). Oxidative stress and cell senescence combine to cause maximal renal tubular epithelial cell dysfunction and loss in an in vitro model of kidney disease. *Nephron Experimental Nephrology*, *122*(3–4), 123–130.

Song, B., Xia, W., Li, T., & Liu, R. H. (2022). Mitochondria are involved in the combination of blueberry and apple peel extracts synergistically ameliorating the lifespan and oxidative stress in Caenorhabditis elegans. *Food & Function*, *13*(15), 8204–8213.

Unsay, J. D., Cosentino, K., Subburaj, Y., & García-Sáez, A. J. (2013). Cardiolipin effects on membrane structure and dynamics. In *Langmuir* (Vol. 29, Issue 51, pp. 15878–15887).

https://doi.org/10.1021/la402669z

Wang, J., Li, T., Li, M., Shi, D., Tan, X., & Qiu, F. (2022). Lycopene attenuates D-galactose-induced insulin signaling impairment by enhancing mitochondrial function and suppressing the oxidative stress/inflammatory response in mouse kidneys and livers. *Food & Function*, *13*(14), 7720–7729.

Wu, X., Chen, Z., Wu, Y., Chen, Y., Jia, J., Shen, N., Chiba, H., & Hui, S.-P. (2022). Flazin as a lipid droplet regulator against lipid disorders. *Nutrients*, *14*(7), 1501.

Yan, X., Chen, X., Fu, C., Jing, C., Zhao, D., & Sun, L. (2022). Ginseng oligosaccharides protect neurons from glutamate-induced oxidative damage through the Nrf2/HO-1 signaling pathway. *Food & Function*, *13*(16), 8605–8615.

Ying, K., Li-Hua, W., Lei, L. I. U., Zheng, L.-H., Yong-Li, B. A. O., Xiu-Xian, L. I. U., Shu-Yue, W., & Zhen-Bo, S. (2021). Immunomodulatory effects of flazin from Crassostrea sikamea on splenic lymphocytes of Sprague-Dawley rats. *Chinese Journal of Natural Medicines*, *19*(11), 836–843.

Zelko, I. N., Mariani, T. J., & Folz, R. J. (2002). Superoxide dismutase multigene family: a comparison of the CuZn-SOD (SOD1), Mn-SOD (SOD2), and EC-SOD (SOD3) gene structures, evolution, and expression. *Free Radical Biology and Medicine*, *33*(3), 337–349.

Zhao, J. Q., Wang, Y. M., Yang, Y. L., Zeng, Y., Wang, Q. L., Shao, Y., Mei, L. J., Shi, Y. P., & Tao, Y. D. (2017). Isolation and identification of antioxidant and α-glucosidase

554 inhibitory compounds from fruit juice of Nitraria tangutorum. *Food Chemistry*, *227*, 93–
555 101. https://doi.org/10.1016/j.foodchem.2017.01.031
556 Zheng, D., Chen, L., Li, G., Jin, L., Wei, Q., Liu, Z., Yang, G., Li, Y., & Xie, X. (2022).
557 Fucoxanthin ameliorated myocardial fibrosis in STZ-induced diabetic rats and cell
558 hypertrophy in HG-induced H9c2 cells by alleviating oxidative stress and restoring
559 mitophagy. *Food & Function*, *13*(18), 9559–9575.
560
561 **Figure Legend**
562 Fig. 1. Effect of BSO and flazin on cell survival. (a) Viabilities of cells treated with BSO and
563 different concentrations of flazin (n = 6). (b) Relative mRNA expression level of *BIK* and
564 *EndoG* (n = 3). Data are presented as means ± SD. Different letters indicated significant
565 differences, $p < 0.05$.
566 Fig. 2. Effect of BSO and flazin on cellular ROS level. (a) Fluorescence staining of cellular
567 ROS (n = 5 - 6). (b) Quantitative analysis of the fluorescence staining of cellular ROS (n = 5 -
568 6). (c) mRNA expression level of *SOD1, SOD2*, and *CAT* (n = 3). Data are presented as means
569 ± SD. Different letters indicated significant differences, $p < 0.05$.
570 Fig. 3. Effect of BSO and flazin on mitochondria. (a) Fluorescence staining of mitochondria
571 and nucleus in cells treated with BSO and flazin (n = 6). (b) Mean length of the mitochondria.
572 (c) Mean network size of the mitochondria. (d) Relative mRNA expression level of *DRP1*,
573 *FIS1*, and *OPA1* (n = 3). Data are presented as means ± SD. Different letters indicated

574 significant differences, $p < 0.05$.

575 Fig. 4. Effect of BSO and flazin on CL profile. (a) Total CL content (n = 3). (b) Total CLOOH
576 content (n = 3). (c) CLOOH to CL ratio (n = 3). (d) Relative content of individual CL species
577 (n = 3). (e) Fatty acyl composition of CL (n = 3). (f) Relative mRNA expression level of *CDS1*,
578 *CDS2*, *PGS1*, and *TAZ* (n = 3). Data are presented as means ± SD. Different letters indicated
579 significant differences, $p < 0.05$.

580 Fig. 5. Effect of BSO and flazin on ATP production and mitochondrial content. (a) ATP
581 production level of cells treated with BSO and flazin (n = 3). (b) Mitochondrial DNA copy
582 number of cells treated with BSO and flazin (n = 3). Data are presented as means ± SD.
583 Different letters indicated significant differences, $p < 0.05$.

Figures

Fig. 1.

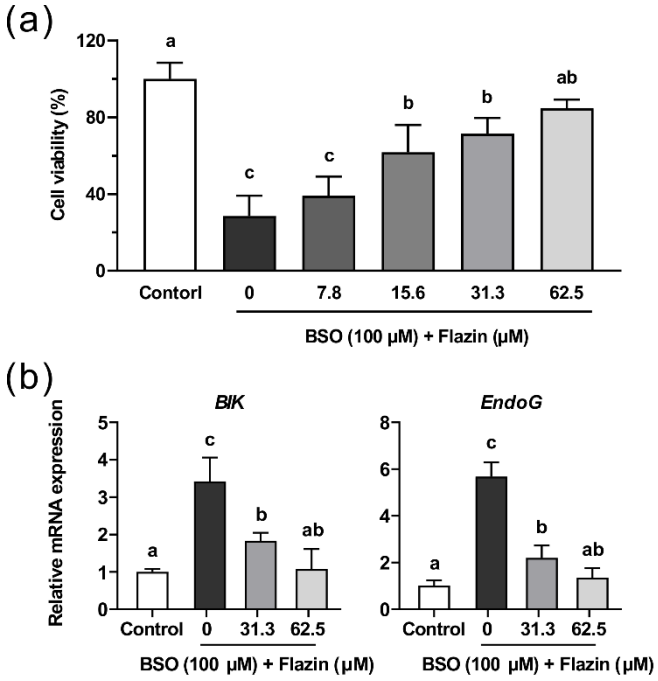

Fig. 2.

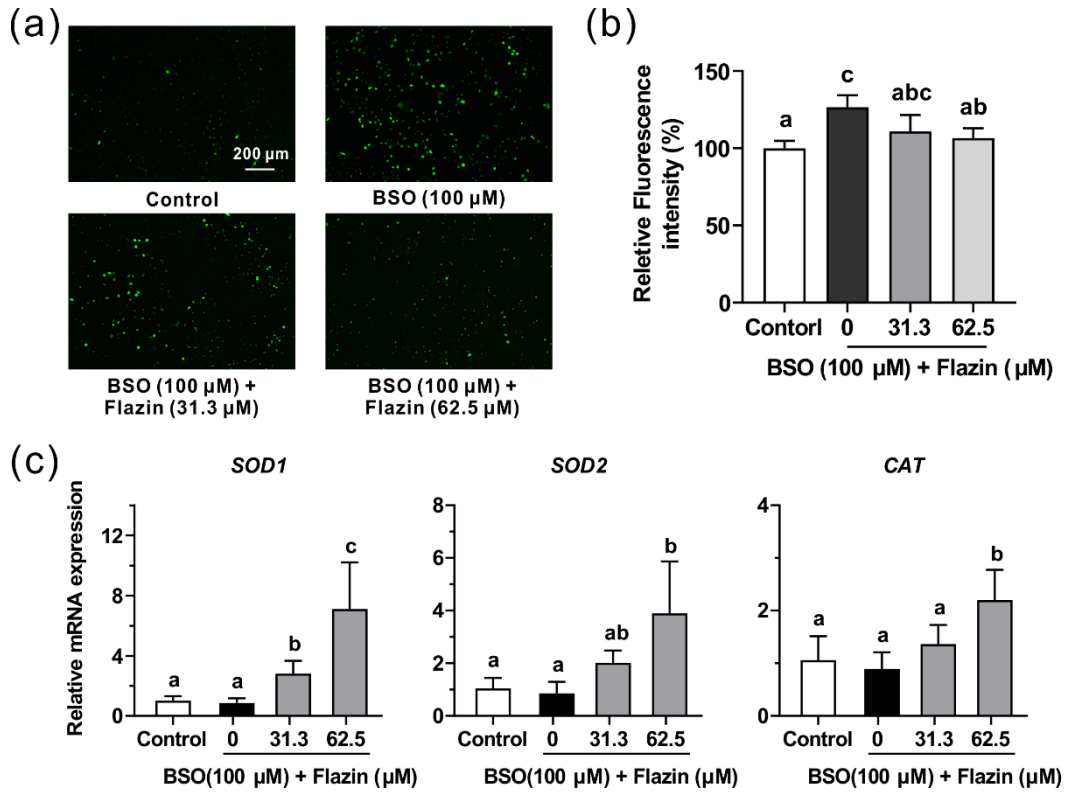
(a)
200 μm
Control
BSO (100 μM)
BSO (100 μM) + Flazin (31.3 μM)
BSO (100 μM) + Flazin (62.5 μM)
(b)
Reletive Fluorescence intensity (%)
150
100
50
0
a
c
abc
ab
Contorl
0
31.3
62.5
BSO (100 μM) + Flazin (μM)
(c)
SOD1
SOD2
CAT
Relative mRNA expression
12
8
4
0
6
2
a
b
c
ab
Control
0
31.3
62.5
BSO(100 μM) + Flazin (μM)

Fig. 3.

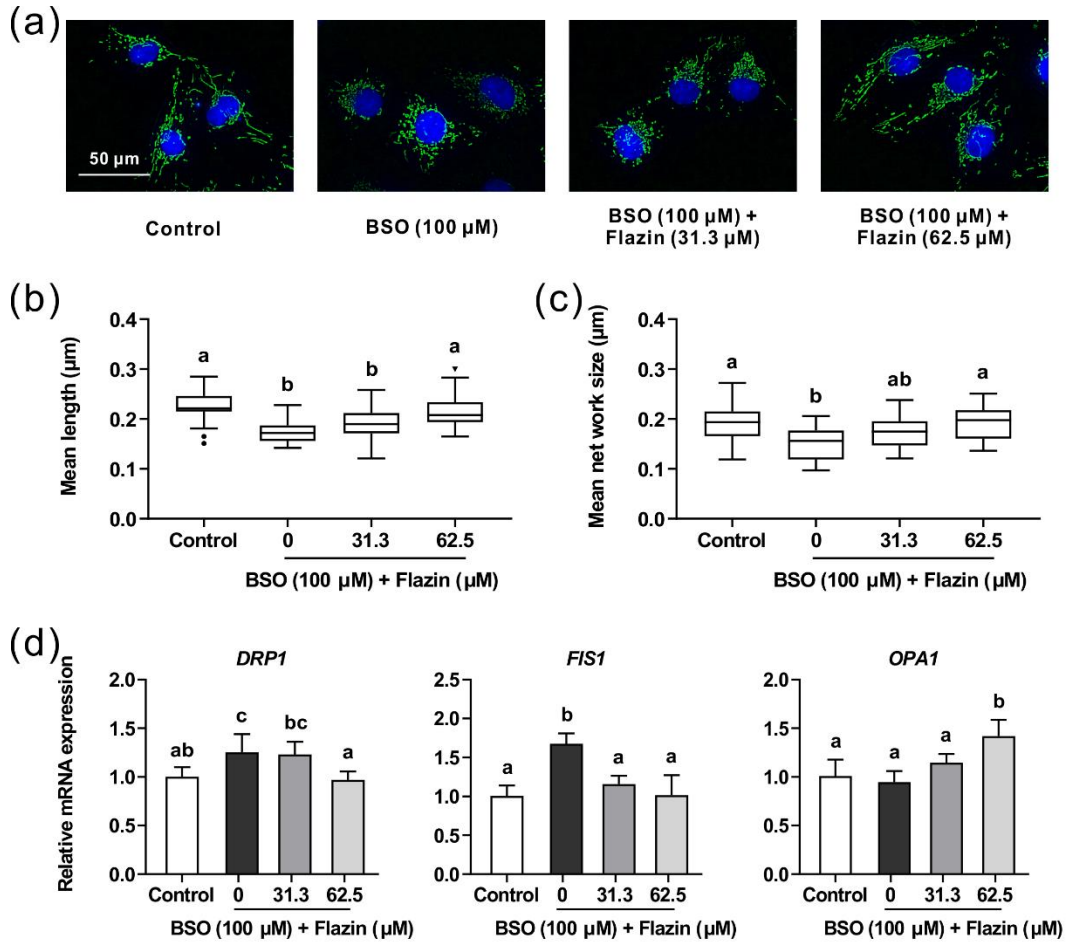
(a)
50 μm
Control
BSO (100 μM)
BSO (100 μM) + Flazin (31.3 μM)
BSO (100 μM) + Flazin (62.5 μM)
(b)
Mean length (μm)
0.0
0.1
0.2
0.3
0.4
a
b
b
a
Control
0
31.3
62.5
BSO (100 μM) + Flazin (μM)
(c)
Mean net work size (μm)
0.0
0.1
0.2
0.3
0.4
a
b
ab
a
Control
0
31.3
62.5
BSO (100 μM) + Flazin (μM)
(d)
Relative mRNA expression
DRP1
0.0
0.5
1.0
1.5
2.0
ab
c
bc
a
Control
0
31.3
62.5
BSO (100 μM) + Flazin (μM)
FIS1
0.0
0.5
1.0
1.5
2.0
2.5
a
b
a
a
Control
0
31.3
62.5
BSO (100 μM) + Flazin (μM)
OPA1
0.0
0.5
1.0
1.5
2.0
a
a
a
b
Control
0
31.3
62.5
BSO (100 μM) + Flazin (μM)

Fig. 4.

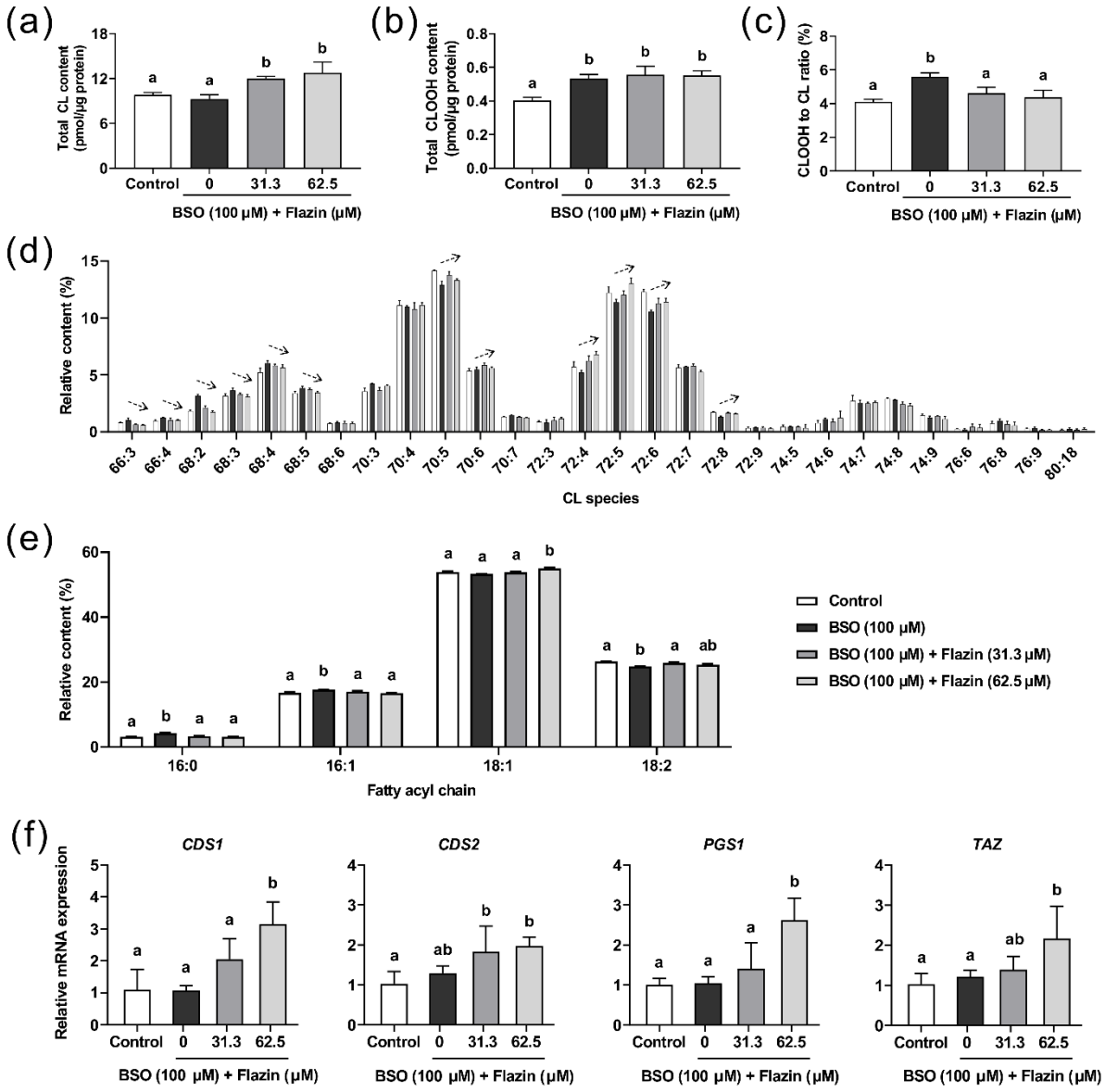
(a)
Total CL content (pmol/μg protein)
Control
0
31.3
62.5
BSO (100 μM) + Flazin (μM)
(b)
Total CLOOH content (pmol/μg protein)
(c)
CLOOH to CL ratio (%)
(d)
Relative content (%)
66:3
66:4
68:2
68:3
68:4
68:5
68:6
70:3
70:4
70:5
70:6
70:7
72:3
72:4
72:5
72:6
72:7
72:8
72:9
74:5
74:6
74:7
74:8
74:9
76:6
76:8
76:9
80:18
CL species
(e)
Relative content (%)
16:0
16:1
18:1
18:2
Fatty acyl chain
Control
BSO (100 μM)
BSO (100 μM) + Flazin (31.3 μM)
BSO (100 μM) + Flazin (62.5 μM)
(f)
Relative mRNA expression
CDS1
CDS2
PGS1
TAZ

Fig. 5.

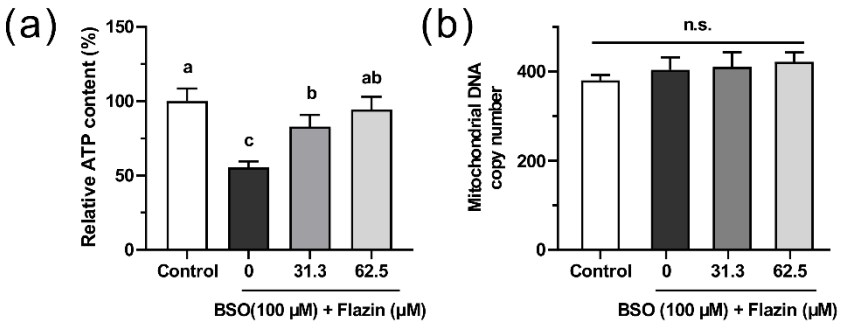
(a)
Relative ATP content (%)
150
100
50
0
a
c
b
ab
Control
0
31.3
62.5
BSO(100 μM) + Flazin (μM)
(b)
Mitochondrial DNA copy number
400
200
0
n.s.
Control
0
31.3
62.5
BSO (100 μM) + Flazin (μM)